Many-body Localization Phase Transition

Atsushi Yamamura
Department of Applied Physics, Stanford University, Stanford, CA 94305
(Dated: June 29, 2020)

Submitted as coursework for PH470, Stanford University, Spring 2020

We introduce several physical quantities as diagnoses of many-body localization phase transition; the relationship between adjacent eigenstates/energies, spatial correlations, and entanglement entropy (EE). These are numerically evaluated by the exact diagonalization (ED). The means of the quantities numerically obtained clearly distinguish the two phases. Furthermore, we show that the normalized variances of the correlation function and EE of half-chain have their peaks at the critical region, and their peaks increase as the system size grows. Further investigation suggests that the variance of EE is primarily dominated by the variance over realizations of the disorder rather than the one over different states or different cuts of the chain. The scaling of these peaks indicates that the system sizes we can access with ED are still in the pre-asymptotic regime far from the fixed point governed by the 'external' randomness. At last, we briefly discuss the possible structure of entanglement in the crossover between the MBL phase and the thermal phase.

I. INTRODUCTION

The notion of localization was first proposed by P.W.Anderson, which deprives many-body systems of ergodicity and prevents it from thermalization. This property emerges in systems with quenched disorders. While Anderson initially analyzed a non-interacting single particle system, many-body localization (MBL) is its generalization by allowing interactions in many-body systems. In this report, we introduce some numerical studies on many-body localization phase transitions, i.e., dynamical phase transition between the MBL phase and the thermal phase. The numerical results shown in the following sections are obtained by us with reference to these papers[1–3].

In the next section, we introduce the model we discuss. Then in the following section, we discuss several principal diagnoses of the transition; the relationship between adjacent eigenstates and energies, spatial correlation function, and entanglement entropy.

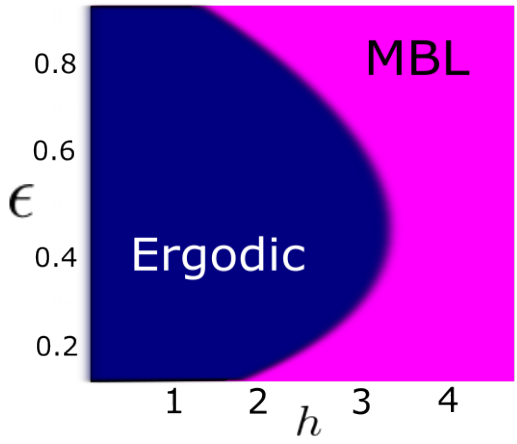

FIG. 1: The rough phase diagram on disorder(h) - energy density(ϵ) space of disordered Heisenberg chain Eq.(1), illustrated based on the numerics in Luitz et al.[2]. The boundary is computed from the finite scalings of various physical quantities with system size $L = 14$ to 22.

II. THE MODEL AND THE NUMERICAL METHOD

We focus on a commonly studied model exhibiting MBL phase transition, a spin-1/2 Heisenberg chain with a random field in the z-direction.

$$H = \sum_{i=1}^{L} h_i S_i^z + \sum_{i=1}^{L-1} \left[S_i^x S_{i+1}^x + S_i^y S_{i+1}^y + S_i^z S_{i+1}^z \right] \quad (1)$$

The field h_i are i.i.d random variables following a uniform distribution on $[-h, h]$.

This model shows MBL phase transition at $h = h_c = 2 \sim 4$, i.e., below h_c, the dynamics of the system is governed by the neighborhood coupling showing ergodicity and converging to thermal equilibrium states. In contrast, above h_c, the system shows localization and fails to thermalize due to the strong disorder. Since this system conserves the total S^z, we restrict our focus only on the symmetric sector of $S^z_{tot} = 0$, which does not affect the properties of the MBL phase transition. For the numerical computation of the physical quantities in the following section, we need the information of eigenvalues and eigenvectors of the Hamiltonian. Thus exact diago-

nalization (ED) is employed. Pal et al.[1] use the middle one-third of the Hamiltonian spectrum gained by ED for their analysis, up to system size $L = 16$. Luitz et al.[2] use a shift-inverted ED method based on a parallel LU decomposition to compute the spectrum around a certain energy level, which allows them to reach $L = 22$. Khemani et al.[3] do not explicitly make mention of their algorithm, but numerically computes physical quantities up to $L = 18$. While the fact that the complexity of the algorithm gets exponentially large as the system size L grows makes it difficult to analyze systems with larger L, we still can observe some signs of the phase transition. Figure(1) shows the rough phase diagram on disorder (h) - normalized energy density (ϵ) space. In the following section, we will discuss the numerical results of several physical quantities that work as signals of the MBL phase transition. Note that the statistical values shown in the following figures are computed over 2000, 2000, 200, 200, or 50 realizations of the disorder h for $L = 8$, 10, 12, 14, 16, respectively.

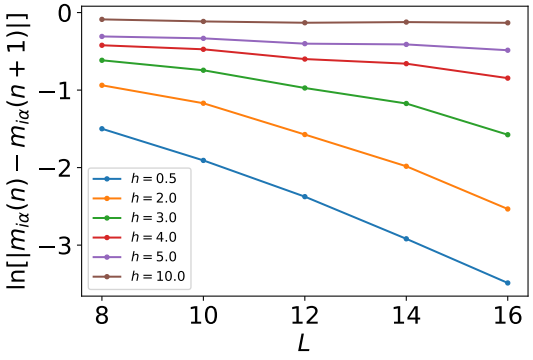

FIG. 2: The natural logarithm of the averaged difference of local magnetization between adjacent eigenstates. The average is taken over eigenstate pairs in the middle one-third of the energy spectrum and over realizations of disorders. These numerical results are computed by Atsushi Yamamura with reference to Pal et al.[1].

III. SIGNALS OF PHASE TRANSITION

A. relationship between adjacent eigenstates and energies

In both phases, the highly excited eigenstates are in the middle of the continuous energy spectrum, and the energy gaps between the adjacent eigenstates are exponentially small. In the thermal phase, the eigenstate thermalization hypothesis holds, and (almost) all eigenstates behave as thermal Gibbs states, which means the eigenstates $|n\rangle, |m\rangle$ with close energy level $E_n \sim E_m$ should show similar expectation values of local observables such as $m_{i\alpha}^{(n)} := \langle S_i^z \rangle_\alpha$ (α is an index representing a sample of disorder). On the other hand, in MBL phase, energy levels are largely governed by disorders h_i, and eigenstates with similar values of $m_{i\alpha}^{(n)}$ usually have energy discrepancy of order $O(h)$ due to the configuration difference in other sites, which is much larger than the exponentially small energy gap between the adjacent eigenstates. This means that the adjacent eigenstates have distinct values of $m_{i\alpha}^{(n)}$. Figure(2) shows the discrepancy of $m_{i\alpha}^{(n)}$ averaged over multiple eigenstate pairs and realizations of the disorder. We can see that in the MBL phase, the difference is independent of system size L, while it drops exponentially in the thermal phase.

Another remarkable feature in the MBL phase appears in its level statistics. Considering the extreme case where h is much larger than the nearest-neighbor coupling, all the eigen-energies are a summation of h_is with certain sign multiplication. Since h_i are i.i.d random variables, the level statistics follows the Poisson distribution, which is unlike the thermal phase following Gaussian-orthogonal ensemble (GOE) level statistics. This distinctive feature of the MBL phase can be well-captured by observing so-called r-ratio

$$r_\alpha^{(n)} := \min\{\delta_\alpha^{(n)}, \delta_\alpha^{(n+1)}\} / \max\{\delta_\alpha^{(n)}, \delta_\alpha^{(n+1)}\} \qquad (2)$$

, where $\delta_\alpha^{(n)}$ is the energy gap between n-th and $n+1$-th energy level of a sample α. The average of this r-ratio converges to ≈ 0.53, ≈ 0.39 in the limit of $L \to \infty$ in the case of GOE statistics, or the Possion distribution, respectively. Figure(3) clearly shows this transition. The crossing points of these curves can be an estimate of the critical point h_c. A noteworthy observation here is that the crossing point gets larger as L grows, which indicates that this transition is happening in the crossover between thermal phase and quantum critical regime, rather than between the MBL phase and quantum critical regime. The other quantities observed by ED method also show this behavior.

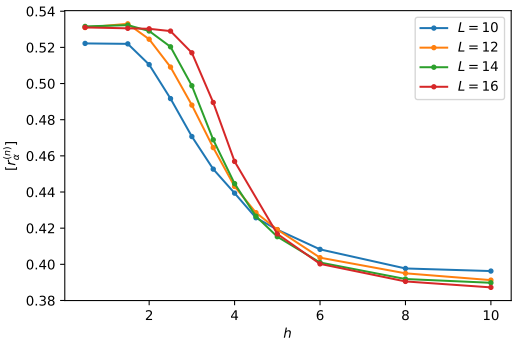

FIG. 3: The r-ratio between adjacent eigenstates averaged over eigenstate pairs in the middle one-third of the energy spectrum and over realizations of disorders. These numerical results are computed by Atsushi Yamamura with reference to Pal et al.[1].

B. spatial correlations

Pal et al. studies spatial correlations to explore the finite-size scaling properties of the MBL transition. Here correlation function $C^{zz}_{n\alpha}(i,j)$ between sites i,j of sample α is defined as follows:

$$C^{zz}_{n\alpha}(i,j) := \langle n|S^z_i S^z_j|n\rangle_\alpha - \langle n|S^z_i|n\rangle_\alpha \langle n|S^z_j|n\rangle_\alpha \quad (3)$$

Figure(4) shows the averaged correlation function $C^{zz}_{n\alpha}(i,i+d)$ as a function of distance d. In the thermal regime, since we are observing highly exited (high temperature) eigenstates, $\langle n|S^z_i|n\rangle_\alpha \approx 0$. Therefore, in the symmetric sector of $S^z_{tot} = 0$, spins are anti-correlated, and we see that $C^{zz}_{n\alpha} \sim L^{-1}$ for spins with adequate distance. This means that logarithm of the correlation is finite even with relatively large d. On the other hand, in the localized regime, we expect that the correlation exponentially drops in the scale of correlation length ζ,

$$C^{zz}_{n\alpha}(i,j) \sim \exp(-|i-j|/\zeta).$$

This agrees with Figure(4), which shows the linear decrease of the correlation function in the log plot.

Pal et al.[1] further computed the spin correlation function with longer distance $L/2$, and analyzed the statistics of the natural logarithm of the averaged correlation function ϕ:

$$\phi = \ln|C^{zz}_{n\alpha}(i,i+L/2)|. \quad (4)$$

Figure(5) shows the difference in the distribution of ϕ between the MBL phase and the thermal phase. It shows that in the thermal phase, it converges to a finite value as L grows, while it has a broad symmetric structure in the MBL phase. In the critical regime between the two, the distribution gets asymmetric and broad.

To analyze the scaling, the authors construct a dimensionless quantity, the normalized standard deviation $\sigma := \sqrt{Var[\phi]}/E[\phi]$. Figure(6) shows it as a function of disorder amplitude h. Due to the asymmetric structure, it has a peak in the critical region, which gets sharp and grows as L increases. The authors argue that this might be an indication that the MBL phase transition might be in an infinite-randomness universality class. As we are going to discuss in the next subsection, this peak of variance can also be seen in entanglement entropy.

C. entanglement entropy

In this subsection, we introduce the behavior of entanglement entropy at the phase transition. In Luitz et al.[2], they computed entanglement entropy (EE) S^E between the left half of the chain and the right half. We expect that EE follows volume law $S^E \sim O(L)$ in the thermal phase, while in the MBL phase, the entanglement decays exponentially and the entropy follows area law $S^E \sim O(1)$. This transition can be seen in Figure(7).

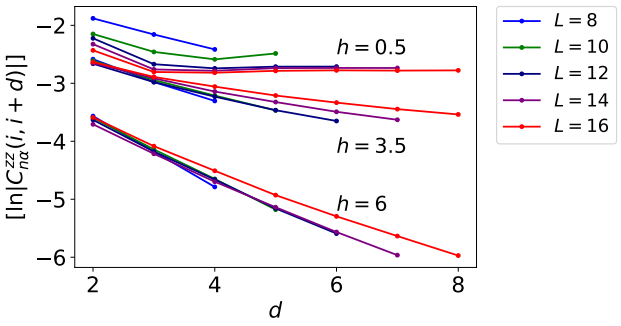

FIG. 4: The averaged spin correlation function $C^{zz}_{n\alpha}(i,i+d)$ in the symmetric sector $S^z_{tot} = 0$, as a function of distance d. It decays exponentially in the localization regime. These numerical results are computed by Atsushi Yamamura with reference to Pal et al.[1].

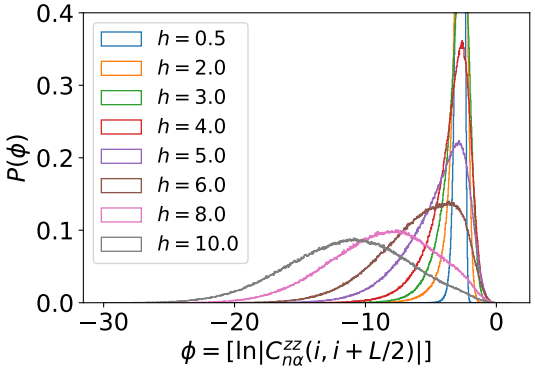

FIG. 5: The probability distribution of the natural logarithm of the averaged correlation function ϕ. The system size here is $L = 16$. These numerical results are computed by Atsushi Yamamura with reference to Pal et al.[1].

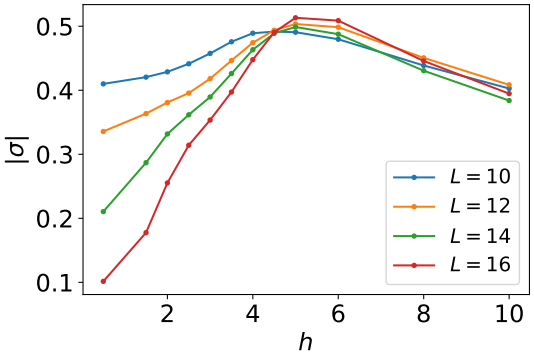

FIG. 6: The normalized standard deviation of ϕ, $\sigma := \sqrt{Var[\phi]}/E[\phi]$ as a function of disorder amplitude h. These numerical results are computed by Atsushi Yamamura with reference to Pal et al.[1].

Here EE is averaged over realizations of the disorder and over 100 eigenstates at the middle of the energy spectrum. In this figure we computed EE up to $L \sim 16$, but they successfully obtained it up to $L \sim 22$, and perform a collapse of S^E/L to the form of $g(L^{1/\nu}(h-h_c))$, by assuming a volume-law scaling at the critical point. The

estimated values of ν and h_c are $\nu \approx 0.8$ and $h_c \approx 3.6$. This value of critical exponent ν apparently violates the Harris criterion $\nu \geq 2d = 2$.

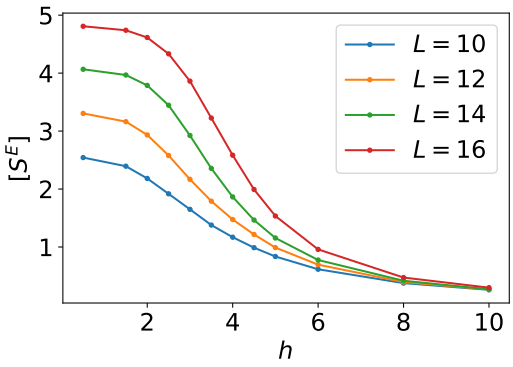

FIG. 7: Entanglement entropy S^E of eigenstates at the middle of the energy spectrum. They are averaged over 100 eigenstates and over realizations of disorders. We can observe the volume-law in the thermal phase, and the area-law in MBL phase.

Khemani et al.[3] further discuss the variance σ_S of EE of half-chains. Specifically, they separately analyzed the variance over different realizations (samples) of disorders, different states, and different cuts of the chain. Figure(8) shows the following three different contributions to the standard deviation of EE.

1. dotted lines: These are obtained by first averaging EE over different cuts of the chain and different eigenstates for each sample of disorder, and then computing the statistics over samples.

2. solid lines: These are obtained by first averaging EE over different cuts for each eigenstate with each sample of disorder, and then computing the standard deviation of the averaged EE over different eigenstates and then averaging the standard deviation over different samples of the disorder.

3. dashed lines: These are obtained by first computing the standard deviation of EE over different cuts, and then averaging it over different eigenstates and different samples of the disorder.

Here the cuts are chosen such that they separate the chain of size L into two chains of size $L/2$, and means and variances are taken across all the possible such cuts. Also, 100 eigenstates at the middle of eigen spectrum are used to compute the statistics across states. The computed standard deviations are divided by $S_T = 0.5[L\ln(2) - 1]$ so that the fraction of EE ranges from 0 to 1. Therefore the y-axis in Figure(8) must not exceed $\frac{1}{2}$ (This maximum is realized when EE follows Bernoulli distribution of 0 or 1 with equal probabilities). The first remarkable fact observed in this figure is that the peak value of the solid line is independent of the system size L, which means the area-law $\sigma_S \sim S_T \sim L$. In contrast, the peak value of the dotted line monotonically grows as L gets large, which suggests a scaling $\sigma_S \sim L^\alpha$ $(\alpha > 1)$. Nevertheless, because the y-axis is $\frac{1}{2}$ at its maximum, it should saturate at larger values of L, and its scaling should be different in the regime. It means that the regime of L reachable by numerical calculations is still pre-asymptotic, and far away from the fixed point dominated by the randomness of the disorder. Therefore it is reasonable that the critical exponent ν gained by numerical analysis breaks Harris criterion.

Finally, the peak of the dashed line appears to be decreasing as L grows, which indicates a scaling $\sigma_S \sim L^\alpha$ $(\alpha < 1)$. As long as this scaling is still valid in the asymptotic regime, Khemani et al.[3] argue that it gives some insight into the entanglement structure of the crossover from the MBL phase to the thermal phase. Specifically, they consider two possible models of the crossover. One is a picture where the system has a small number of long contiguous thermal or localized blocks, which gives a subthermal but volume-law EE. The other model is the one with a long sparse entangled cluster, which consists of many small thermal blocks with various degrees of entanglement. Following the first picture, the half-chain EE is strongly influenced by whether the cut is in the thermal or localized block, which probably gives a bimodal distribution and its standard deviation scales $\sim L$. In contrast, the alternative picture tells us that EE depends on how many spins belonging to the sparse entangled cluster the half-chain has, and if the number of spins in the cluster is order of N, the standard deviation of the number of those spins in the half-chain scales $\sim N^{1/2}$, which suggests that the standard deviation of EE also scales $\sim N^{1/2}$. Therefore the authors claim that this picture matches the result shown in Figure(8) rather than the first picture.

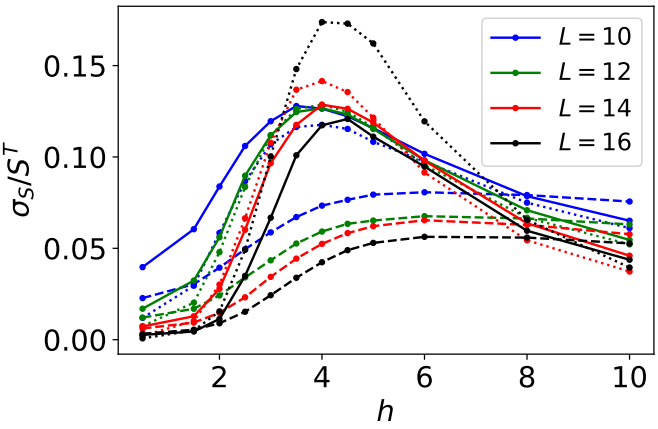

FIG. 8: Standard deviation of entanglement entropy of half-chain σ_S divided by the random pure state value S^T. dashed lines, solid lines, and dotted line represent contributions of cut-to-cut, eigenstate-to-eigenstate, and sample-to-sample variations, respectively. These numerical results are computed by Atsushi Yamamura with reference to Khemani et al.[3].

IV. SUMMARY

In this report, we introduced the many-body localization phase transition observed in the spin-1/2 Heisenberg model with random fields along the z direction and discussed several critical physical quantities as signals of the phase transition, based on the numerical computations. The first remarkable transition between the two phases can be seen in the relationship between adjacent eigenstates in the energy spectrum. In the thermal phase, adjacent eigenstates have almost equivalent expectation value of local magnetization, and the statistics of energy difference follows the one of GOE. In contrast, in the MBL phase, adjacent eigenstates have different values of local magnetization, and the level statistics follow the Poisson distribution. In addition to these quantities, we also introduced statistics of spatial quantities: the spin correlation function and half-chain entanglement entropy. They both work as a diagnosis of the transition. The averaged correlation function decays exponentially as a function of distance in the MBL phase in contrary to the thermal phase. The averaged entanglement entropy follows the volume-law (area-law) in the thermal phase (the MBL phase), respectively. Moreover, we report that the normalized standard deviation of these two quantities shows a peak at the critical region. Further analyses show that the contribution of this variance is mostly from the one over different realizations. The peak of the variance grows monotonically and does not show the behavior of saturation, which should be able to be observed in the asymptotic regime. This fact indicates that the accessible system size L is still in the pre-asymptotic regime far from the fixed point governed by the 'external' randomness. In these computations, we need to rely on exact diagonalization, which makes it challenging to deal with a larger L. At last, we briefly discussed the possible model of the entanglement structure of crossover from the MBL phase to the thermal phase.

[1] A. Pal and D. A. Huse, "Many-body localization phase transition" Phys. Rev. **82**, 174411 (2010).

[2] D. J. Luitz, N. Laflorencie, and F. Alet, "Many-body localization edge in the random-field Heisenberg chain" Phys. Rev. B**91**, 081103 (2015).

[3] V. Khemani, S. Lim, D. Sheng, and D. A. Huse,"Critical Properties of the Many-Body Localization Transition" Phys. Rev. X **7**, 021013 (2017).